Springer

Journal of Mechanical Science and Technology 23 (2009) 1428~1434

Journal of Mechanical Science and Technology

www.springerlink.com/content/1738-494x
DOI 10.1007/s12206-008-1219-6

Analysis of dynamic characteristics for vibration of flexural beam in ultrasonic transport system †

G.H. Kim[1], J.W. Park[1] and S.H. Jeong[2,*]

[1]*Department of Mechanical Engineering, Graduate School, Chosun University, Gwangju, 501-759, Korea*
[2]*Department of Mechanical Engineering, Chosun University, Gwangju, 501-759, Korea*

(Manuscript Received July 24, 2008; Revised August 25, 2008; Accepted December 22, 2008)

Abstract

An object transport system is an essential device in the factory automation system (FAS). Generally, an object transport system is driven by a conveyor belt system or a magnetic levitation system. However, contact force in the conventional transport system can damage precision optical components, while the magnetic field can destroy the inner structure of the semiconductor. The ultrasonic transport system transports objects on an elastic body using an ultrasonic wave. When an ultrasonic wave is applied to a flexural beam, the flexural beam vibrates to excite the air layer, which lifts up the object on the beam to transport. In this paper, the dynamic characteristics of the ultrasonic transport system are theoretically analyzed. Through normal mode expansion, the modeling equation for steady state response of ultrasonic vibration is expressed and the natural frequency of the flexural beam in each mode is also estimated by using the finite element method (FEM).

Keywords: Ultrasonic wave; Vibration; Traveling wave; Standing wave; Flexural beam

1. Introduction

With the recent advancements in the semiconductor and information technology industries, the need has arisen for a system that can transport semiconductors and optical elements without damage. If their surfaces are damaged by a magnetic field or contact force during transport, semiconductors and optical elements become defective. To overcome this problem, a transport system that conveys objects using ultrasonic levitation is being studied.

Actuators using ultrasonic waves were developed in the early 1990s in the USA and Japan. In 1982, Sashida proposed an ultrasonic actuator called "traveling-wave motor", and Ro studied an object transport system that used an ultrasonic wave. So far, most studies have been conducted for the purpose of reducing motor noises[1].

In this paper, the dynamic characteristics of ultrasonic transport system are theoretically identified using normal mode expansion. The Euler-Bernoulli beam theory is applied to observe the natural frequency of the flexural beam and to estimate the progressive frequency for transporting the object. Also, the natural frequency of the flexural beam is verified by using the finite element method.

2. Standing wave and traveling wave

The vibration that occurs on the surface of the flexural beam when an ultrasonic wave is applied takes either the form of a standing wave or a traveling wave. A standing wave is generated by superposition of two harmonic waves with the same amplitude and frequency but moving in different directions and is expressed by the following equation:

† This paper was recommended for publication in revised form by Associate Editor Eung-Soo Shin
*Corresponding author. Tel.: +82 62 230 7178, Fax.: +82 62 230 7178
E-mail address: shjeong@chosun.ac.kr

$$A\sin(kx-\omega t) + A\sin(kx+\omega t) = 2A\cos(\omega t)\sin(kx) \quad (1)$$

where, k = wave number and ω = angular frequency

A standing wave projected on a plane of length (x) and time (t) of the flexural beam at its vibration amplitude is illustrated in Fig. 1. By connecting lines with the same amplitude, a uniform profile is formed. Standing waves maintain simple harmonic motion in one place as time goes on.

A traveling wave projected on a plane of length (x) and time (t) of the flexural beam at its vibration amplitude is illustrated in Fig. 2. In this figure, a band of uniform strips with the same amplitude and inclination are formed. Here, when the inclination is positive, the direction of traveling wave is expressed with (→); and when the inclination is negative, it is expressed with (←).

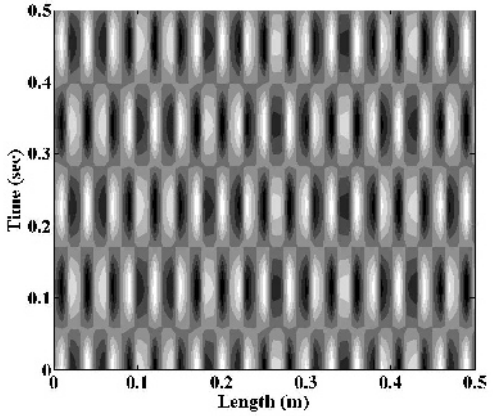

Fig. 1. Standing wave.

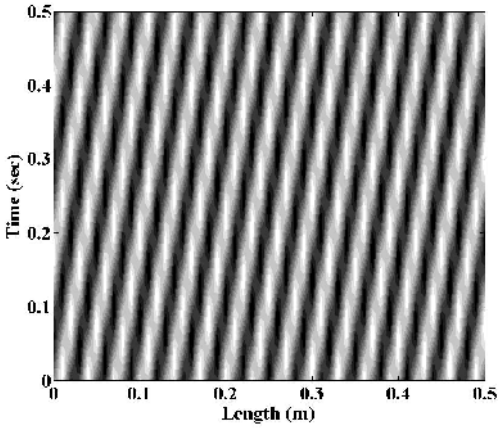

Fig. 2. Traveling wave.

A traveling wave can be expressed with two standing waves as shown below:

$$\begin{aligned}&\cos(kx-\omega t) \quad (2)\\ &= \cos(kx)\cos(\omega t) + \cos(kx-\pi/2)\cos(\omega t-\pi/2)\\ &\quad \sin(kx-\omega t)\\ &= \sin(kx)\cos(\omega t) - \cos(kx)\sin(\omega t)\end{aligned}$$

According to Eq. (2), a traveling wave is generated by superposition of two standing waves with a phase difference of 90°.

3. Design of ultrasonic transport system

The ultrasonic transport system consists of a function synthesizer, power amplifiers to amplify the generated function, ultrasonic wave generators, and a flexural beam to generate a traveling wave and serve as a transport guide, as shown in Fig. 3[2, 3]. Each of the ultrasonic wave generators used for Channels 1 and 2 consists of a piezoelectric actuator, a booster, and a conical horn. The flexural beam has a rectangular section. The conical horn is fastened to the flexural beam with a bolt at a position other than the nodal line. Duralumin 7072 is used for the flexural beam material due to its excellent acoustic properties[4].

In this paper, when an object moves in the direction from Channel 2 to Channel 1, the direction is marked + (positive direction) and when it moves in the opposite direction, it is marked – (negative direction).

4. Traveling wave of ultrasonic transport system

4.1 Theoretical analysis

It is assumed that deformation of an elastic body

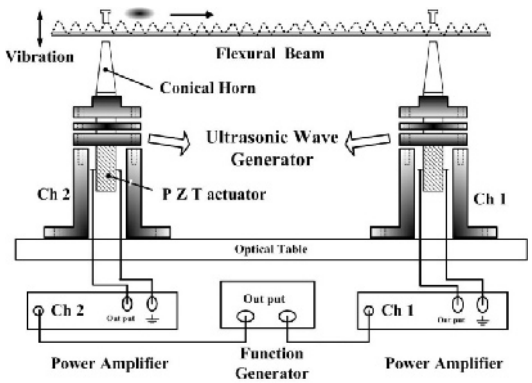

Fig. 3. Layout of object transport system.

such as a beam, plate or shell is approximated by a simple geometric equation, and material points on a straight line in the thickness direction of the elastic body remain on the same straight line after the deformation. To determine the modeling equation for vibration displacement of the flexural beam, either the Euler-Bernoulli theory without consideration of shear effect or the Timoshenko theory with consideration of shear effect is used. Generally, when the length-thickness ratio of the beam is 20:1 or larger, the Euler-Bernoulli beam theory is applied and, when it is smaller than 10:1, the Timoshenko beam theory is applied.

In this paper, Euler-Bernoulli beam theory is used with the following assumptions to observe a modeling equation for vibration displacement of the flexural beam:

- The material of the beam is homogeneous and isotropic;
- Hook's law is obeyed;
- Energy dissipation (due to damping) is initially ignored and the vibrational amplitudes are small; and
- There are no shear forces in the beam, and no bending moments acting upon it.

The Euler beam equation for the transverse bending vibration of a beam can be expressed as follows:

$$\frac{\partial^4 u}{\partial x^4}+\frac{\rho A}{EI}\frac{\partial^2 u}{\partial t^2}=0 \tag{3}$$

where, u(x, t) : vibration displacement of transverse direction
ρ : mass density of the beam
A : cross-sectional area
EI : flexural stiffness of the beam

The prototype beam model for the ultrasonic transport system is shown in Fig. 4. The flexural beam is connected to the horn that excites the ultrasonic wave at the positions of $l_1$and l_2.

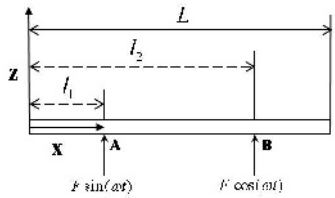

Fig. 4. Beam model of prototype.

To calculate u(x,t), the displacement in the z-axis direction, of the flexural beam after t (seconds) at a position x (displacement) away in the length direction, the method of separating variables was applied to separate the variables into ϕ, a function of position, and q(t), a function of time. The boundary conditions of the flexural beam with free-free ends were used to obtain the solution for the mode shape ϕ. The initial conditions were applied to evaluate the time-dependent Fourier coefficients and determine the contribution of each mode to the total responses. The general solution for displacement in the transverse direction, which occurs on the flexural beam, was obtained by the superposition of all modes. In this paper, we observed the modeling equation as shown in Eq. (4) using two dominant mode shapes closest to the excitation frequency(ω). Each equation in the bracket indicates one traveling wave, and the modeling equation is expressed as the sum of two traveling waves[5-8].

$$\begin{aligned} u(x,t) &= [A\sin(k_{30}x-\pi/4)\cos(\omega t)+B\sin(k_{31}x-\pi/4)\sin(\omega t)] \\ &+[C\sin(k_{31}x-\pi/4)\cos(\omega t)+D\sin(k_{30}x-\pi/4)\sin(\omega t)] \end{aligned} \tag{4}$$

$$A=\frac{2F\phi_{30}(l_1)}{\sqrt{\rho a}(\omega_{30}^2-\omega^2)} \qquad B=\frac{2F\phi_{31}(l_2)}{\sqrt{\rho a}(\omega_{31}^2-\omega^2)}$$

$$C=\frac{2F\phi_{31}(l_1)}{\sqrt{\rho a}(\omega_{31}^2-\omega^2)} \qquad D=\frac{2F\phi_{30}(l_2)}{\sqrt{\rho a}(\omega_{30}^2-\omega^2)}$$

4.2 Natural frequency of flexural beam

The finite element method was applied for modal analysis of the flexural beam. The input conditions for the finite element analysis are listed in Table 1. Con-

Table 1. Input conditions for FEM analysis.

		Flexural Beam
Mesh	Mesh Type	Solid Mesh
	Element Size	0.003 m
	Nodes	5534
	Elements	668
Properties (Duralumin 7072)	Elastic Modulus	6.8×10^{10} Pa
	Poisson's Ratio	0.33
	Density	2720 kg/m^3
Boundary Condition	Constraint	(- , 0 , -) in 2 surfaces

Table 2. Natural frequency of flexural beam.

n th mode	Frequency (kHz)	
	Theoretical	FEM
26	19.1	19.5
27	20.6	20.9
28	22.1	22.4
29	23.7	23.9
30	25.3	25.5
31	27.0	27.1
32	28.7	28.7

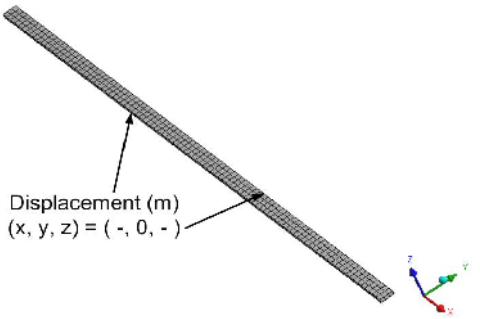

Fig. 5. Modeling of flexural beam.

sidering the displacement in the transverse direction of the flexural beam, the two side surfaces of the flexural beam were constrained by the slide condition as shown in Fig. 5.

For free-free end conditions of the beam, the shear force and the bending moment are defined as 0 by the boundary condition, so that the frequency equation can be expressed as follows:

$$\cosh(k_B l) \cdot \cos(k_B l) = 1 \quad (5)$$

where, $k_B l$: point of intersection curves $\cos(k_B l)$ and $1/\cosh(k_B l)$.

The natural frequency of the flexural beam is calculated as follows:

$$\omega_n = \frac{(k_B l)^2}{l^2}\sqrt{\frac{EI}{\rho A}} \quad (6)$$

The natural frequencies of the flexural beam obtained by finite element analysis and those obtained by applying Eq. (6) are listed in Table 2. The natural frequencies obtained by Euler-Bernoulli beam theory agree well with those obtained by applying the finite

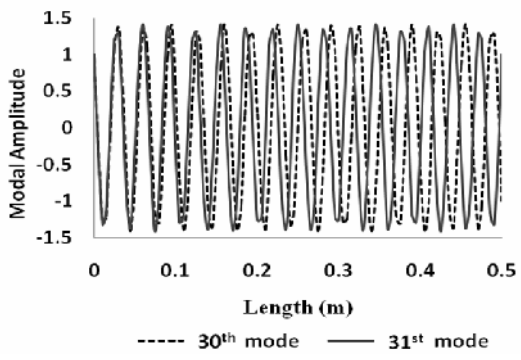

Fig. 6. 30th and 31st mode shape.

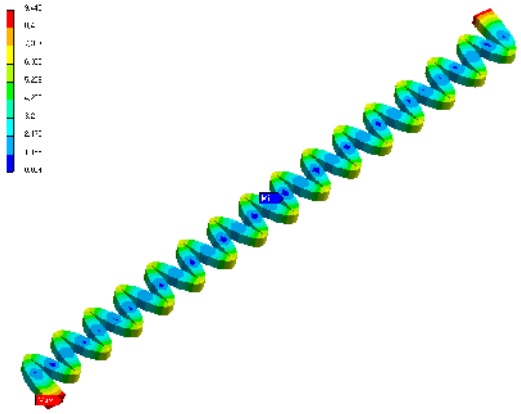

(a) 25.5kKz

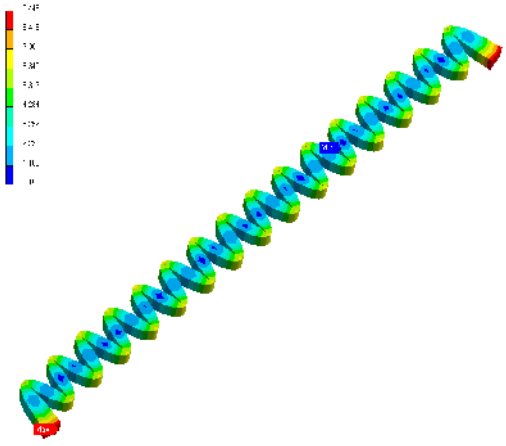

(b) 27.1kHz

Fig. 7. Frequency mode of flexural beam.

element analysis. The 30th and the 31st normal modes are illustrated in Fig. 6, and the mode shape of the flexural beam is shown in Fig. 7.

Table 3. Wave propagation direction in several simulation conditions.

n^{th}	Frequency (kHz)			A	B	wave propagation direction	C	D	wave propagation direction
	ω_n	ω_{n+1}	ω						
29	23.7	25.3	24.5	+	+	→	-	+	→
30	25.3	27.0	26.2	+	-	←	-	-	←
31	27.0	28.7	27.9	+	+	→	-	+	→
32	28.7	30.5	29.6	+	-	←	-	-	←

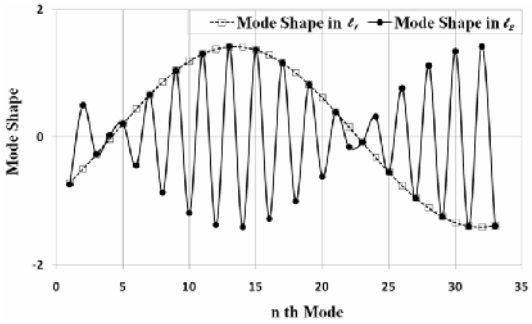

Fig. 8. Mode shape in l_1 and l_2.

4.3 Change of transport direction according to frequency

The direction of wave propagation was determined by the n^{th} mode shape at Positions l_1 and l_2. The n^{th} mode shape of the flexural beam is as follows:

$$\phi_n(x) = \sin(k_{B_n} x) - \cos(k_{B_n} x) \quad (7)$$

The mode shape according to k_i is illustrated in Fig. 8. As the mode shape in l_1 had a negative value in 30^{th} and 31^{st} modes, $Ø_{30}(l_1)$ and $Ø_{31}(l_1)$ had negative values. As the mode shape in l_2 changed its sign according to the mode, $Ø_{30}(l_2)$ had a positive value and $Ø_{31}(l_2)$ had a negative value. Therefore, it was possible to estimate the wave propagation direction.

To simulate the wave propagation direction, Matlab was used to simulate the conditions of the 30^{th} mode with an excitation frequency of 26.2 kHz. The wave propagation direction was estimated by using the two flexural beam resonance frequencies closest to the excitation frequency. To verify the wave propagation direction at the 30^{th} and 31^{st} simulation conditions, the vibration amplitude was projected onto the time plane for the beam length as shown in Fig. 9 and 10. For the 30^{th} simulation, the wave propagates in (←) direction by A and B and in (←) direction by C and D as shown in Fig. 9(a) and (b). For the 31^{st} simulation, all waves propagated in (→) direction, both by A and B and by C and D as shown in Fig. 10(a) and (b).

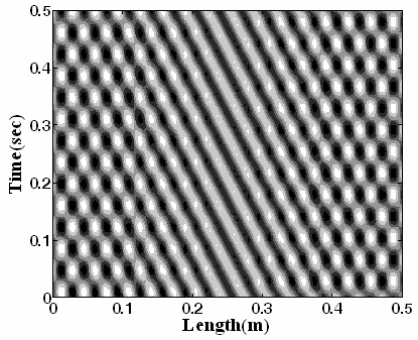

(a) Wave caused by A and B

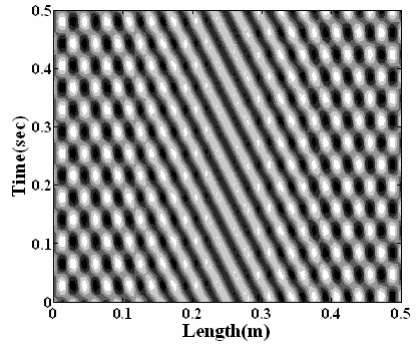

(b) Wave caused by C and D

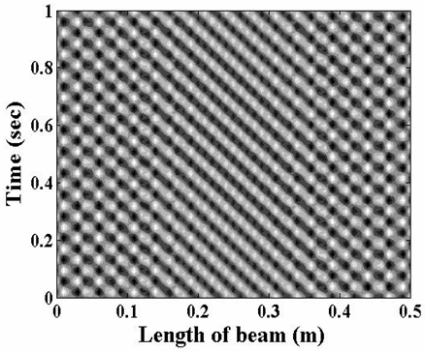

(c) Wave caused by A, B, C and D

Fig. 9. Wave in 30^{th} simulation condition.

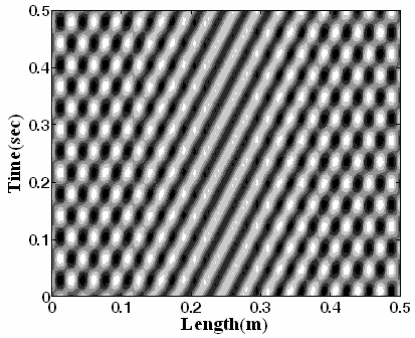

(a) Wave caused by A and B

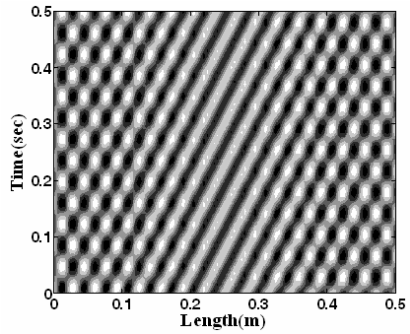

(b) Wave caused by C and D

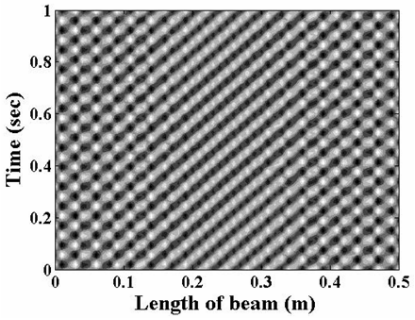

(c) Wave caused by A, B, C and D

Fig. 10. Wave in 31st simulation condition.

The simulation results are summarized in Table 3. The excitation frequency regularly changed the signs of A, B, C and D, and the wave propagation direction of u(x,t) is determined by combination of the wave propagation direction by A and B and that by C and D. For example, when the wave propagation direction by A and B is (→) and that by C and D is (→), the wave of u(x,t) also propagates in (→) direction. If the propagation directions are opposite, a standing wave occurs instead of a traveling wave.

To measure the transport direction of an object according to frequencies, an experiment was conducted in which frequencies were changed from 26.5kHz to

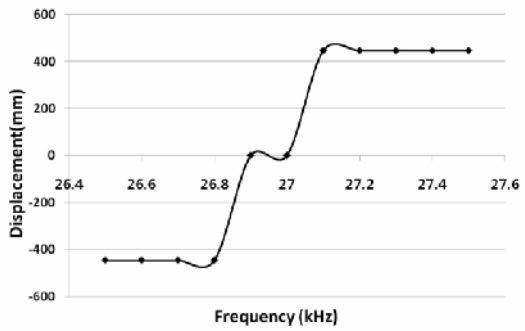

Fig. 11. Transporting displacement of object according to frequency.

27.5kHz at an interval of 100Hz. As shown in Fig. 11, the object was transported in (-) direction from 26.5kHz to 26.8kHz and in (+) direction from 27.0kHz to 27.5kHz. At 27.0kHz, the flexural beam resonance frequency, the object was not transported.

Table 3 shows that the wave propagates in (←) direction when excited with 26.2kHz and in (→) direction when excited with 27.9kHz. This result proves that the wave propagation direction changes according to the flexural beam resonance frequency at 27.0kHz.

5. Conclusions

The dynamic characteristics of the ultrasonic object transport system were theoretically analyzed. The natural frequency of the flexural beam was found and a position that fastened a conical horn to the flexural beam was confirmed by using the finite element method. Matlab was used to simulate the wave propagation direction, and the vibration amplitude was projected onto the time plane for the beam length to verify the wave propagation direction of the 30th and 31st simulation conditions. A modeling equation for the steady state flexural vibration of the beam is induced by superposing two modes near the excitation frequency. The excitation frequency changed the signs of coefficients A, B, C and D in the modeling equation for the flexural beam, and the wave propagation direction changed according to the signs of coefficients A, B, C and D in the modeling equation. To check the results of the theoretical analysis, an experiment was conducted with changing frequency; this experiment confirmed that the wave propagation direction changed at 27.0kHz. Therefore, the simulation result agreed well with the experiment result.

Acknowledgment

This study was supported by research funds from Chosun University, 2008.

References

[1] E. Matsuo, Y. Koike, K. Nakamura, S. Ueha and Y. Hashimoto, Holding characteristics of planar objects suspended by near-field acoustic Levitation, *Ultrasonics 38*, (2000) 60-63.

[2] S. H. Jeong, G. H. Kim, S. B. Choi, K. R. Cha and S. Song, A study on the transportation characteristics according to beam shape of optical lens transport system using ultrasonic wave, *Journal of the Korean Society of Machine Tool Engineering*, (2006) 8-14.

[3] S. H. Jeong, H. U. Kim, K. R. Cha, S. B. Choi and S. Song, A study on the Dynamic Characteristics of object transport system using ultrasonic wave, *Journal of the Korean Society for Precision Engineering*, (2005) 151-158.

[4] S. H. Jeong, G. H. Kim, S. B. Choi, J. H. Park and K. R. Cha, A study on an object transport system using ultra wave excitation, *Journal of Mechanical Science and Technology*, (2007) 941-945.

[5] B. G. Loh and P. I. Ro, 2000, Changing the propagation direction of flexural ultrasonic progressive waves by modulating excitation frequency, *Journal of Sound and Vibration,* Vol. 238, No. 1, North Carolina State University, (2000) 171-178.

[6] M. P. Norton, *Fundamentals of Noise and Vibration Analysis for Engineers,* Cambridge, (1989) 81-98.

[7] S. S. Rao, *Mechanical Vibrations,* Addison-Wesley, England, (1995) 609-622.

[8] S. Ueha, Y. Tomikawa, M. Kurosawa and N. Nakamura, *Ultrasonic Motors,* Oxford, England, (1993) 9-17.

Sang-Hwa Jeong received his M.S. degree in Mechanical Engineering from KAIST, Korea, in 1985 and his Ph.D. degree from North Carolina State University, USA, in 1992. Dr. Jeong is currently a professor at the department of Mechanical Engineering of Chosun University in Gwangju, Korea. His research fields are micro-actuator design, ultrasonic transport system, and SMA actuator of robot finger.